

E. Ahedo, P. Martínez Cerezo and J.M. Gallardo  
*E.T.S.I. Aeronáuticos, Univ. Politécnica, 28040 Madrid, Spain*

M. Martínez-Sánchez  
*Dep. of Aeronautics & Astronautics, M.I.T., Cambridge, MA 02139*

*A recently completed 1-D, macroscopic model of the plasma flow in a Hall thruster is here used to stand out that the solutions inside the thruster channel and in the external plume are always coupled and conditions at the channel exit can change significantly with thruster parameters and external conditions. In addition, preliminary results on a modified model which includes heat conduction are presented.*

## 1. INTRODUCTION

A recent paper by us[1] presents a complete derivation of a 1-D stationary model of the plasma flow structure in a Hall thruster. It includes the plasma response both inside the thruster channel and in the external plume. In particular, the plume is modelled as a 1-D jet of divergent area which intersects a neutralization surface (i.e. a virtual cathode) of the ion beam. This plume model, although simple, allowed us i) to close in a consistent way the problem and ii) to have an approximate picture of the external plasma response. Indeed, the main flaw of the model was inside the channel, around the ionization layer, where too high temperatures were obtained. Heat conduction and losses to lateral walls are the two effects neglected in the model, that are expected to reduce that temperature peaks.

In this conference paper we focus on two subjects. First, we emphasize the strong coupling between the plasma behavior inside and outside the channel, and how conditions at the channel exit depend on that coupling. This issue is crucial to give reliability to more refined models of the plume (like Ref. [2] and others) which in general do not include a proper matching with the plasma flow in the channel. Second, we report the first results we have obtained on heat conduction effects on the plasma structure.

## 2. THE MODEL

Geometrical sketches of the thruster and the main features of our 1-D model are drawn in Fig. 1. The main hypotheses of the model are well discussed elsewhere[1]. The axial profile of the radial magnetic field is assumed Gaussian. The channel is of length  $L$  and radial area  $A_c$ . Electrons are injected into the plume at a surface (point P) placed at a distance  $L_{EP}$  from the channel exit (point E). The voltage difference between anode (point A) and point P is the discharge voltage  $V_d$ , and the

electron current delivered at that surface is the discharge current  $I_d$ . One part of this current diffuse inwards across the magnetic field lines and ionizes the mass flow of neutrals,  $\dot{m}$ , injected at the anode. The other part flows outwards and neutralizes the ion current; subscript  $\infty$  will refer to downstream conditions far away from the cathode. The plasma is considered quasineutral everywhere except in a thin electron-repelling sheath attached to the anode (region AB in Fig. 1, with  $x_B \simeq x_A = 0$  in the quasineutral scale). The sheath potential,  $\Phi_{sh} = \Phi_B - \Phi_A > 0$ , balances the thermal flow collected at the anode to the diffusion flow of electrons in the quasineutral channel.

The stationary, macroscopic equations for the quasineutral plasma between point B(entrance to the anode sheath) and the external point P are

$$\frac{1}{A} \frac{d}{dx} (An_e v_i) = \frac{1}{A} \frac{d}{dx} (An_e v_e) = -\frac{1}{A} \frac{d}{dx} (An_n v_n) = n_e \nu_i, \quad (1)$$

$$\frac{1}{A} \frac{d}{dx} (Am_i n_e v_i^2) = -en_e \frac{d\Phi}{dx} + \nu_i m_i n_e v_n, \quad (2)$$

$$\frac{1}{A} \frac{d}{dx} (Am_i n_n v_n^2) = -\nu_i m_i n_e v_n, \quad (3)$$

$$0 = -\frac{d}{dx} n_e T_e + en_e \frac{d\Phi}{dx} - \nu_d m_e n_e v_e, \quad (4)$$

$$\frac{1}{A} \frac{d}{dx} A \left( \frac{3}{2} T_e n_e v_e + Q_e \right) = -n_e T_e \frac{dv_e}{dx} + \nu_d m_e n_e v_e^2 - \nu_i n_e \alpha_i E_i, \quad (5)$$

$$\frac{dT_e}{dx} = -\frac{2m_e \nu_d}{5n_e T_e} Q_e, \quad (6)$$

Here, for a complete listing of symbols and variables see Ref.[1]; the law for the evolution of the radial area  $A(x)$  along the plume will be formulated later;  $\nu_i = n_n R_i(T_e)$  is the ionization frequency; the effective axial diffusion frequency for the magnetized electrons is  $\nu_d$  satisfies

$$\nu_d \simeq \omega_e^2 / \nu_e \quad (7)$$

with  $\omega_e$  the electron gyro-frequency and  $\nu_e = \nu_{en} + \nu_{ei} + \alpha_B \omega_e$  the total collision frequency, which adds contributions from electron-neutral and electron-ion collisions, and from the anomalous Bohm diffusion (in the classical formulation it is  $\alpha_B \sim 1/16$ );  $v_e$  and  $Q_e$  mean the axial components only of the electron velocity and heat conduction flux. The azimuthal components of these magnitudes verify

$$v_{e\theta}/v_e \simeq Q_{e\theta}/Q_e \simeq -\omega_e/\nu_e, \quad (8)$$

Notice that the above diffusive model for the electrons is based in two assumptions:

$$|\mathbf{v}_e| \ll \sqrt{T_e/m_e}, \quad v_e \ll \omega_e. \quad (9)$$

The model of Ref. [1] assumed  $Q_e = 0$  instead of Eq.(6).

## 2.1 Singular/sonic points

Solving for all spatial derivatives we obtain a matrix relation of the form

$$(1 - M^2) \frac{d\mathbf{Y}}{dx} = \mathbf{F}(\mathbf{Y}), \quad \mathbf{Y} = (n_e, v_i, T_e, \dots) \quad (10)$$

where  $\mathbf{Y} = (n_e, v_i, T_e, \dots)$  groups the 8 plasma variables,

$$M = \frac{v_i}{\sqrt{T_e/m_i}} \quad \text{for } Q_e \neq 0$$

$$M = \frac{v_i}{\sqrt{5T_e/3m_i}} \quad \text{for } Q_e = 0 \quad (11)$$

and  $\mathbf{F}$  is a regular function (different for the zero and non-zero conduction models). Equation (10) shows that  $M$  can be assimilated to a Mach number for the ion fluid so that singular points of the mathematical model can be interpreted as sonic points of the ion beam. Since a sonic/supersonic expansion of the ion beam into the vacuum a sonic point (point S with  $M_S = 1$ ) must be expected in the channel. We will see below that there is a second singular point at the transition to the anode sheath (point B), for the ion back-flow.

From the mathematical point of view, notice that heat conduction is not just another effect included into the zero-conduction model. It leads to a different mathematical model, with an extra differential equation and different singular points. This new model cannot be solved from parametric continuation on the zero-conduction model and has required a completely new integration.

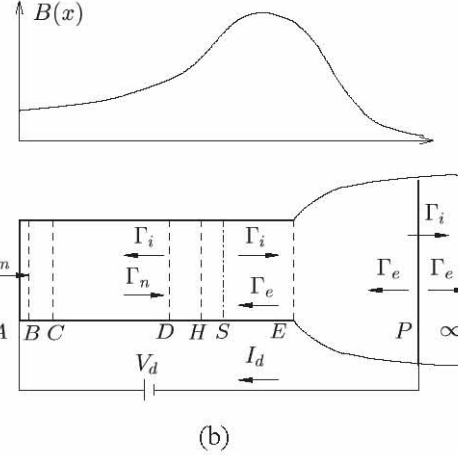
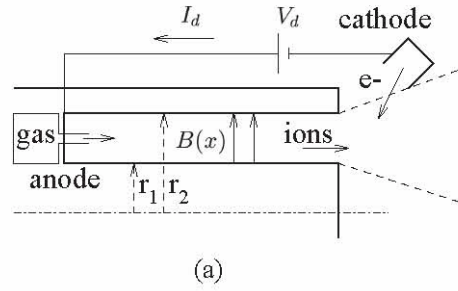


**Figure 1.-** Sketches of (a) the Hall thruster and (b) the 1-D macroscopic model.  $\Gamma_\alpha$ ,  $\alpha = i, e, \dots$  are particle flows of the different species. Surface  $P$  is the cathode (beam neutralizer).

## 2.2 The anode sheath

The continuity of the (small) diffusive electron flow of the channel into the anode requires the formation of an electron repelling sheath tied to the anode (region AB). The needed sheath potential is

$$\frac{e\Phi_B}{T_{eB}} = \ln \frac{\bar{c}_e B}{4|v_{eB}|} > 0, \quad (12)$$

where  $\bar{c}_e = \sqrt{8T_e/\pi m_e}$  and we took the arbitrary origin of  $\Phi$  at point A.

Since all ions are provided from ionization in the thruster, plasma quasineutrality and the cold-ion condition ( $T_i/T_e \ll 1$ ) imply the back-flow of ions in the rear part of the channel. This explains that the Bohm condition at the transition from the quasineutral plasma into the non-neutral sheath reads

$$M_B = -1. \quad (13)$$

Finally, it is readily seen that the heat flow deposited by the electrons into the sheath (at point B) is

$$Q_{eB} = n_e v_e T_e \left( \ln \frac{\bar{c}_e}{4|v_e|} - \frac{1}{2} \right) \Big|_B. \quad (14)$$

### 2.3 Boundary and plume conditions

Equations (1)-(6) require eight boundary conditions distributed between points B and P, plus an equation for the area variation of the quasi 1-D external plume,  $A(x)$ . Following the experimental results of Pollard and Beiting[3] we assume that the boundary lines in the near plume expands radially with constant speed. This at the channel exit can be taken as the local sound speed of the ion flow at the channel exit,  $v_{iE}/M_E$ . Thus, if  $h(x)$  is the crescent radial width of the cylindrical plume, and  $\delta$  the semi-angle of divergence, the cross-area variation in the plume satisfies

$$\frac{d}{dx} \ln A = \frac{2}{h} \tan \delta = \frac{2v_{iE}}{hM_E v_i}. \quad (15)$$

Five boundary conditions are set at point B:

i)-iii) Eqs. (12)-(14).

iv)-v) The injected flow of neutrals,  $\dot{m}$ , and their velocity,  $v_{nA}$ , are known.

The other three boundary conditions are:

vi) The discharge voltage  $V_d$  is known and is equal to the potential difference between anode and the virtual cathode:  $\Phi_P = -V_d$  (for  $\Phi_A = 0$ ).

vii) The electron temperature at the the virtual cathode,  $T_{eP}$ , is known.

viii) The expansion of the ion beam into the external, rarefied atmosphere is either choked or supersonic. For a choked-exit solution, one just sets

$$M_E = 1. \quad (16)$$

Instead, for a supersonic-exit solution, a regular sonic point [point S in Fig. 1] exists inside the channel, which satisfies[1]

$$\left. \frac{dv_i}{dx} \right|_S = v_i - \frac{v_i}{T_e} \frac{G}{1 - M^2} \Big|_S \text{ finite} \quad (17)$$

at  $M_S = 1$ , which means  $G_S = 0$  with

$$G = -\nu_d m_e v_e - \nu_i \left[ \frac{3}{5} m_i (2v_i - v_n) - \frac{(2/5)\alpha_i E_i + T_e}{v_e} \right] + \frac{3}{5} m_i v_i^2 \frac{d \ln A}{dx} \quad (18)$$

for the zero-conduction model and

$$G = -\nu_d \left[ m_e v_e - \frac{2m_e Q_e}{5n_e T_e} \right] - \nu_i m_i (2v_i - v_n) + m_i v_i^2 \frac{d \ln A}{dx} \quad (19)$$

for the non-zero conduction model.

The discharge current  $I_d$  is part of the solution. For a supersonic exit, the position of point S,  $x_S$ , must be determined also. For both types of solutions, discontinuities in the plasma derivatives are expected at point E.

## 3. DISCUSSION OF SOLUTIONS

### 3.1. Types of stationary solutions

Details of the numerical algorithm used to integrate plasma equations are omitted. We just point out the most relevant aspects. First, for a supersonic-exit solution, a Taylor expansion of the plasma equations is required to determine the derivatives at point S. This makes point S the most convenient point to start an initial-value integration. Second, not every set of 'initial parameters' at point S yields a valid solution between points B and S. A first restriction to the 'initial parameters' comes from the condition that the plasma flow be accelerating at point S:  $G_{S-} \leq 0$ . The second restriction comes from the observed fact that there are solutions departing from  $S^-$  towards B, which never reach a negative ion velocity and finish instead in a singular point with  $M = +1$ ; these solutions have no physical meaning in a conventional Hall thruster.

A third restriction, is that the ion back-flow must accelerate towards the anode, that is  $G_B > 0$ . This condition implies a restriction to the non-zero conduction model exclusively. This is readily seen from Eqs.(18) and (19). At point B, ionization is practically negligible so only the terms corresponding to  $\nu_d$  matter. Then, Eq.(18) assures that  $G_B > 0$  always, while  $G_B > 0$  in Eq.(19) only for

$$\frac{2Q_e}{5n_e T_e v_e} \Big|_B < 1. \quad (20)$$

Using Eqs.(12)-(14), it turns out that valid solutions in the conduction model are restricted to

$$0 < \ln \frac{\bar{c}_{eB}}{4|v_{eB}|} < 3. \quad (21)$$

Figures 2(a) and (b) illustrate, for the no-conduction model, the parametric regions of the different solutions between points B and S. Parameters

$$\eta_i = \frac{m_i A n_e v_i}{\dot{m}}, \quad i_d = \frac{m_i I_d}{e \dot{m}} \quad (22)$$

are the (local) ionization fraction and the discharge current ratio, respectively. For  $i_d > 1$ , four parametric regions are found: *region 1*, with  $G_{S-} > 0$ , and *region 2*, with  $G_{S-} < 0$  and  $\eta_{iB} > 0$ , are regions of non physical solutions; *region 3*, with  $G_{S-} < 0$  and  $\eta_{iB} < 0$ , corresponds to the *choked-exit regime*; and (line) *region 4*, with  $G_S = 0$  and  $\eta_{iB} < 0$ , corresponds to the *supersonic-exit regime*. For the choked-exit regime (point S = point E), only solutions with  $G_{S+} > 0$  positive are acceptable. The limit line  $G_{S+} = 0$  for two values of the channel radial width is depicted in

Fig. 2. Region 4 of supersonic-exit solutions can be divided in high and low ionization branches. The low-ionization branch yields propellant utilizations well below 50% and corresponds, then, to inefficient thruster operation. The high-ionization branch is actually a near-total ionization branch and corresponds to the near-complete ionization mode referred by Morozov[4]. For  $i_d \leq 1$ , the high-ionization branch disappears.

Therefore, there are three types of stationary solutions: with choked exit, with supersonic exit and high ionization, and with supersonic exit and low ionization. And the point to notice here is that each of them leads to different conditions at the channel exit. In addition, there are restrictive bounds for a stationary solution to exist, which can explain some of the oscillatory behaviors observed experimentally.

The equivalent of Fig. 2 for the conduction model has not been computed yet.

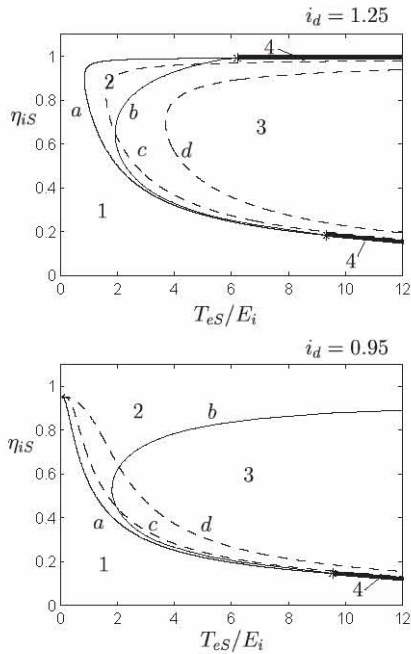


**Figure 2.-** Regions leading to different types of solutions between points S and B for a constant B-profile. Line *a* corresponds to  $G_S^- = 0$ ; line *b* to  $\eta_{iB} \rightarrow 0$ ; lines *c* and *d* to  $G_S^+ = 0$  for two radial widths of the channel. Region 2 is between lines *a* and *b*; region 4 (supersonic-exit regime) corresponds to the thick parts of line *a*, to the right of the intersections (asterisks) with line *b*. (Taken from Ref.[1])

### 3.2. Structure of the plasma flow

Figure 3 shows a solution of the non-conduction model with supersonic exit and high ionization, for parameters typical of SPT-100 (see Ref. [1] for details). As in the experiments of Ref.[5] the plasma

structure consists mainly of i) an upstream diffusion region, with predominant ion motion towards the anode, negligible electric field, no ion production, a low plasma temperature, and the pressure gradient driving the electrons; ii) an intermediate intense ionization layer, with peaks of the plasma density and temperature ; and iii) a region of ion acceleration, which extends into iv) the plume. The potential drop is distributed among the last three regions.

Figure 4 shows a solution of the conduction model for conditions similar to those of Fig. 3. Notice that the plasma structure is similar but the maximum temperature (and pressure) have been reduced significantly. The diffusion region is much smaller but Fig. 4 is only a preliminary result, not entirely satisfactory; for instance, the peak of temperature should be closer to point S and the ionization layer. Computations are underway to understand how different parameters affect the spatial profiles and the performance.

### 3.3. Performances and channel/plume coupling

Figures 5 to 8 show for the non-conduction model the influence of different control parameters on the thrust, defined as

$$F = m_i(\Gamma_i v_i)_E + (p_E - p_\infty)A_c,$$

and on two parameters at the channel exit: the electron temperature and the ion beam velocity. For this model, the potential at point E satisfies[1]

$$\Phi_A - \Phi_E \simeq m_i v_{iE}^2 / 2e \quad (23)$$

approximately. Notice that  $L$  and  $B_{max}$  can be considered channel parameters whereas  $V_d$  and  $L_{EP}$  are related to plume design. A relevant observation is that all points in Figs. 5 to 8 correspond to the regime of supersonic exit and near-total ionization, and the changes in  $v_{iE}$  and  $T_{eE}$  are important already. Variations of these parameters are for sure larger if we could draw the change to a stationary regime with lower ionization or choked exit.

## 4. CONCLUSIONS

Using the non-conduction model of Ref.[1] we have tried to demonstrate that for the solution of a plume model to be reliable a correct matching with the plasma flow in the channel is essential. The two channel and plume problems are always coupled. Plasma conditions in the upstream boundary of the plume are affected by i) the regime of the plasma flow in the channel, ii) design parameters of the thruster, and iii) plume boundary conditions.

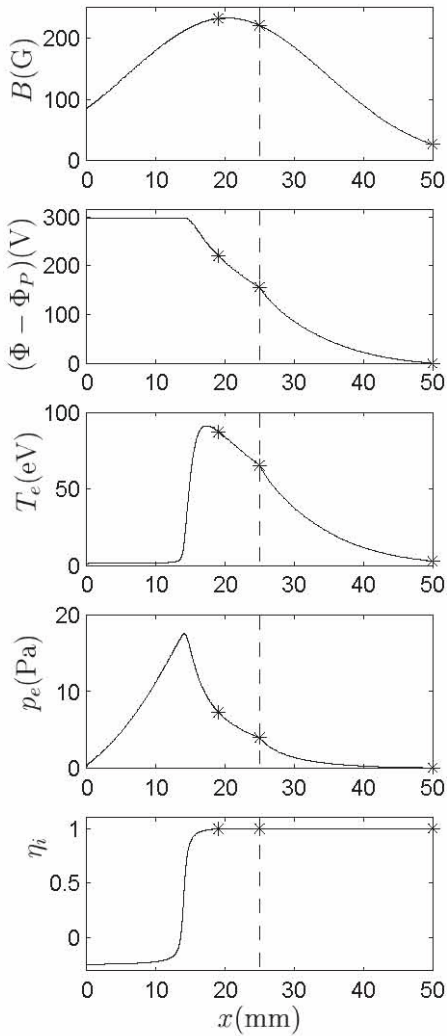


**Figure 3.-** Zero conduction model. Example of plasma response. (Taken from Ref.[1])

Also, we have presented our first results on a non-zero heat conduction model. This model has required a totally new integration with respect to the non-conduction model. Differences in the singular/sonic points, boundary conditions and restrictions have pointed out. The model offers the desired softening of the temperature profile but further research on the adequate control parameters is necessary.

### ACKNOWLEDGMENTS

The work of E. Ahedo was financed partially by the Dirección General de Enseñanza Superior e Investigación Científica of Spain, under project PB97-0574-C04-02, and in part by the USAF European Office for Aerospace Research and Development (EOARD) under contract F61775-00-WE034. The participation of P. Martínez-Cerezo and J.M. Gallardo was made possible thanks to the EOARD contract exclusively.

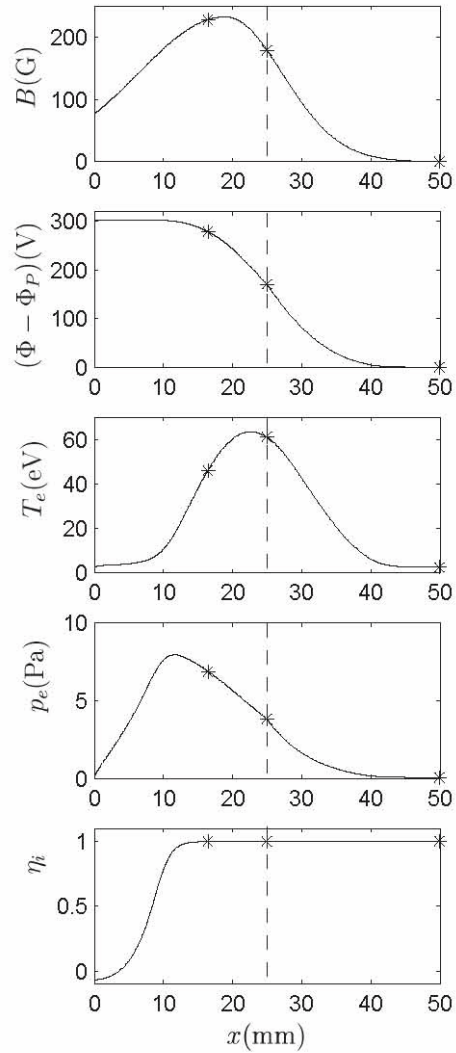


**Figure 4.-** Non-zero conduction model. Example of plasma response.

### References

- [1] E. Ahedo, P. Martínez-Cerezo, and M. Martínez-Sánchez. to appear in *Phys. Plasmas*, 8(6), 2001.
- [2] I.D. Boyd, L. Garrigues, J. Koo, and M. Keidar. In *36th Joint Propulsion Conf., Huntsville, AL*, AIAA Paper No. 2000-3520, 2000.
- [3] J.E. Pollard and E.J. Beiting. In *SP-465: 3rd Spacecraft Propulsion Conference*, (ESA Publications Division, Noordwijk, 2000), pages 789–796.
- [4] A.I. Morozov, Y.V. Esipchuk, G.N. Tulinin, A.V. Trofimov, Y.A. Sharov, and G.Y. Shchepkin. *Soviet Phys.-Tech. Phys.*, 17(1):38–45, 1972.
- [5] A.M. Bishaev and V. Kim. *Sov. Phys. Tech. Phys.*, 23(9):1055–1057, 1978.

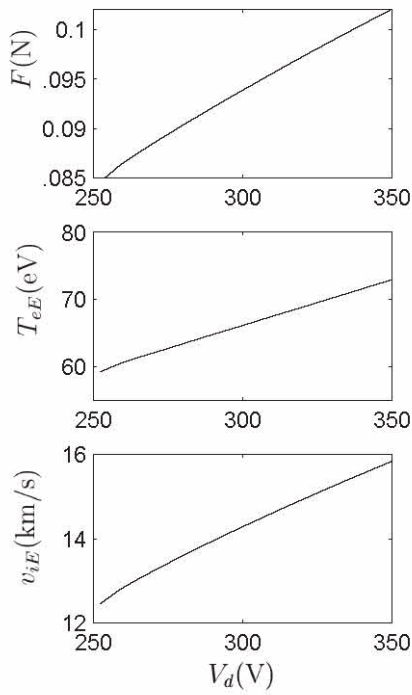


**Figure 5.-** Influence of discharge voltage on performance and parameters at channel exit.

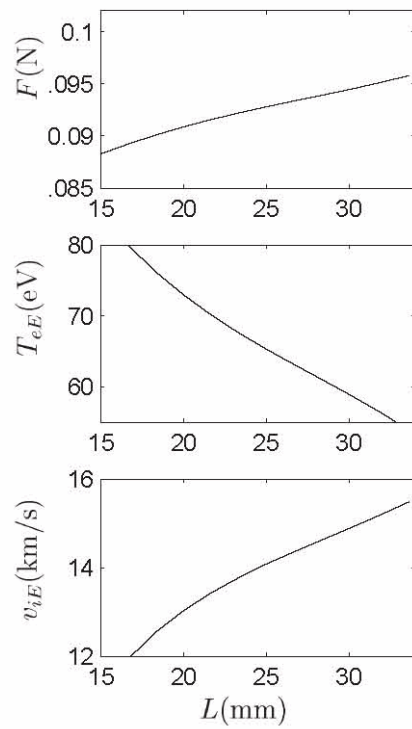


**Figure 7.-** Influence of the channel length on performance and parameters at channel exit.

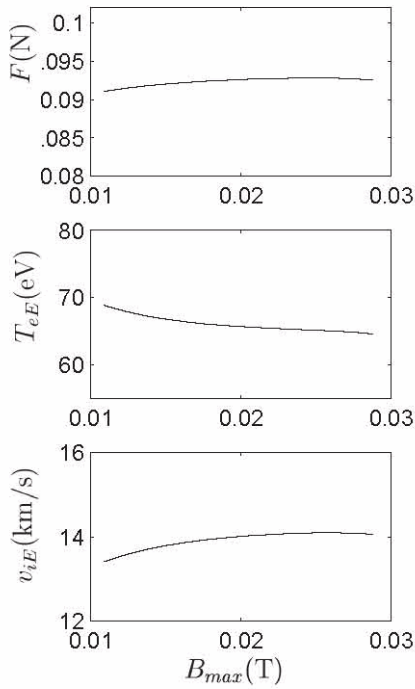


**Figure 6.-** Influence of the maximum of the magnetic field on performance and parameters at channel exit.

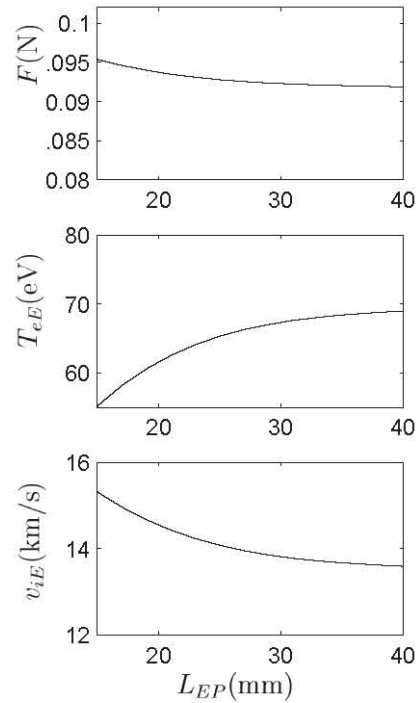


**Figure 8.-** Influence of the position of the neutralization surface on performance and parameters at channel exit.

